

Mechanical Properties of Neuronal Growth Cone Membranes Studied by Tether Formation with Laser Optical Tweezers

Jianwu Dai and Michael P. Sheetz

Department of Cell Biology, Duke University Medical Center, Durham, North Carolina 27710 USA

ABSTRACT Many cell phenomena involve major morphological changes, particularly in mitosis and the process of cell migration. For cells or neuronal growth cones to migrate, they must extend the leading edge of the plasma membrane as a lamellipodium or filopodium. During extension of filopodia, membrane must move across the surface creating shear and flow. Intracellular biochemical processes driving extension must work against the membrane mechanical properties, but the forces required to extend growth cones have not been measured. In this paper, laser optical tweezers and a nanometer-level analysis system were used to measure the neuronal growth cone membrane mechanical properties through the extension of filopodia-like tethers with IgG-coated beads. Although the probability of a bead attaching to the membrane was constant irrespective of treatment; the probability of forming a tether with a constant force increased dramatically with cytochalasin B or D and dimethylsulfoxide (DMSO). These are treatments that alter the organization of the actin cytoskeleton. The force required to hold a tether at zero velocity (F_0) was greater than forces generated by single molecular motors, kinesin and myosin; and F_0 decreased with cytochalasin B or D and DMSO in correlation with the changes in the probability of tether formation. The force of the tether on the bead increased linearly with the velocity of tether elongation. From the dependency of tether force on velocity of tether formation, we calculated a parameter related to membrane viscosity, which decreased with cytochalasin B or D, ATP depletion, nocodazole, and DMSO. These results indicate that the actin cytoskeleton affects the membrane mechanical properties, including the force required for membrane extension and the viscoelastic behavior.

INTRODUCTION

Cell migration is an important component of metastasis, invasion, the immune response, and development. During migration, the plasma membrane is distorted by the mechanical forces of the motility process (Vasiliev, 1985; Trinkaus, 1985). The role of the membrane is largely passive in responding to cytoskeletal deformations (Sheetz, 1993), although previously an active role through a membrane flow had been postulated (Bretscher, 1989). In the case of growth cone migration, the axon must elongate, increasing the plasma membrane area dramatically (Popov et al., 1993). Even if the membrane is passive, the growth cone must work against the load that membrane distortion produces. Consequently, the mechanical properties of the cell membranes contribute to the cell deformability and movement. Understanding the mechanical properties of growth cone membranes will help us better understand cell migration at a fundamental level.

Several experimental methods have been used to investigate mechanical properties of cell membranes (Hochmuth et al., 1973; Evans and Skalak, 1979; Pasternak and Elson, 1982; Bray et al., 1986; Bo and Waugh, 1987). Using these methods, the mechanical properties of liposomes, sea urchin eggs, erythrocytes, and lymphocytes have been studied.

However, they are applicable mainly to suspension cells and are inapplicable to cells with complex cell structure such as neuronal cells. The interpretation of the membrane contribution in many such measurements is complicated by the fact that the cytoskeleton is also deformed in a major way. To circumvent the direct cytoskeletal contribution, membranous tethers lacking a continuous cytoskeleton have been studied in erythrocytes and pure lipid bilayers. From these studies, the static and dynamic components of the membrane mechanical properties were determined. The static tension on tethers contains contributions from the in-plane tension (Hochmuth and Evans, 1982a; Waugh, 1982a) and the bending stiffness of the bilayer, which is highly curved in the tethers (Waugh and Hochmuth, 1987). When tethers are elongated, a viscous force is introduced that contains contributions from the membrane viscosity and the interbilayer shear as the lipids flow onto the tether. The fluid nature of such tethers indicates that they are largely membranous, and the absence of spectrin or actin in erythrocyte tethers has shown that even the membrane skeleton is depleted (Berk and Hochmuth, 1992). Nevertheless, cytoskeleton can influence the formation of tethers as evidenced by the differences between erythrocytes and pure lipid vesicles. Perhaps even the tether mechanical properties would be modified by alterations of the cytoskeleton.

In motile cells and particularly in the forward portion of migrating cells, actin filament assembly and disassembly is intimately tied to motility (reviewed in Sheetz, 1994; Zigmond, 1993; Cooper, 1991). Further, actin and actin-binding proteins such as spectrin are closely associated with plasma membranes in virtually all cells, including neurons (Bennett, 1990). The support of plasma membranes by the

Received for publication 22 August 1994 and in final form 28 November 1994.

Address reprint requests to Dr. Michael P. Sheetz, Department of Cell Biology, P.O. Box 3709, Duke University Medical Center, Durham, NC 27710. Tel.: 919-684-8091; Fax: 919-684-8592; E-mail: mike_sheetz@cellbio.duke.edu.

© 1995 by the Biophysical Society

0006-3495/95/03/988/09 \$2.00

membrane skeleton is extensive in the erythrocyte but in other cells glycoproteins can diffuse over micron distances before encountering barriers to lateral diffusion (de Brabander et al., 1991; Edidin et al., 1991). The barriers to lateral diffusion have not been identified, but when glycoproteins become anchored to the cytoskeleton, they are generally anchored to the actin filaments. Actin is consequently closely apposed to the plasma membrane and may have an important role in determining the membrane properties. Because tether formation involves the separation of membrane from most of the membrane skeleton, there should be dramatic effects of the actin cytoskeleton on the probability of tether formation. We will therefore probe the effect of actin depolymerization on tether formation and tether mechanical properties.

Previous work (Ashkin and Dziedzic, 1989; Wayne et al., 1991) found that the laser trap could produce sufficient force to pull membranous tethers from cell surfaces. Optical tweezers allow exquisitely fine control of position (~ 10 nm for trap beam stability) and of forces (~ 0.1 pN resolution) on a wide range of particle sizes (25 nm to 25 μm) in a noninvasive manner (Svoboda and Block, 1994; Kuo and Sheetz, 1992). The laser tweezers were developed for the microscopic manipulation of cells and organelles with a minimum of damage (Ashkin, 1970; Ashkin and Dziedzic, 1987, 1989; Ashkin et al., 1987). They have been used for a variety of applications, including the measurement of membrane barriers (Edidin et al., 1991, 1994), the force of single motor molecules (Kuo and Sheetz, 1993; Svoboda et al., 1994; Finer et al., 1994), and regional specializations in cell membranes (Kucik et al., 1991; Schmidt et al., 1994).

We now extend those studies to determine the membrane mechanical properties from the forces applied to the beads for different velocities of tether elongation. With nanometer-level motion analysis, the instantaneous force on the tether can be measured. In addition, we can evaluate the relative strength of the membrane-skeleton interaction from the probability of tether formation at a given force on the bead. We measured the mechanical properties after treatment by the cytochalasins, DMSO, ethanol, nocodazole, and ATP depletion. These treatments altered the membrane-cytoskeleton interaction and affected the membrane mechanical properties. The method we described here for determining membrane mechanical properties with the laser tweezers can be generally applied under a variety of different conditions.

MATERIALS AND METHODS

Cell culture

Chick dorsal root ganglion (DRG) explants were dissected from 12-day chick embryos and plated in the growth wells on treated coverslips. To prepare the cell growth wells, 20 \times 20 mm (No. 1) glass coverslips (BDL, Lincoln Park, NJ) and 10-mm-diameter cloning cylinders (Bellco, Vineland, NJ) were cleaned by soaking in 20% nitric acid for 2–3 h, followed by rinsing in distilled water for 1 h. Then they were put into 95% ethanol overnight and rinsed in distilled water for at least 2 h. After drying and sterilization, a cloning cylinder was secured to the coverslip with sterilized silicone grease to form a growth well. The growth well was coated with

0.01% poly-L-lysine for 15 min at room temperature, rinsed 3 times with sterilized water, then dried in a sterile hood. Just before the dissection, poly-L-lysine-coated growth wells were exposed to a 1:50 Matrigel (Collaborate Research, Bedford, MA):MEM solution. Explants were maintained at 37°C, 5% CO₂ in clear MEM (Gibco BRL, Grand Island, NY) supplemented with the following: 20 mM HEPES, 6 mg/ml glucose, 5 μM /ml pen./strep., 2 mM L-glutamine, 10 μM /ml N2 Serum-free supplement (Gibco), and 10 nM/ml nerve growth factor (NGF 2.5s; Gibco). The explants were used after they were incubated for 24–48 h.

Bead preparation

In previous studies, we observed that covaspheres coated with a control IgG preparation would bind to growth cone membranes without any apparent perturbation of growth cone behavior. To prepare IgG-coated beads, rat IgG (Sigma Chemical Co., St. Louis, MO) was solubilized at a concentration of 10 mg/ml in PBS. Then, 50 μl of covaspheres (0.5 μm , Duke Scientific, Palo Alto, CA) was added to 50 μl of the above IgG solution and was incubated at 4°C overnight. The beads were pelleted by centrifugation at 2000 \times g and 4°C for 10 min. Then the beads were resuspended in 1 mg/ml BSA-PBS solution, rinsed by pelleting and resuspension with MEM medium 3 times and resuspended in 100 μl of MEM medium. For the experiments, the bead solution was diluted 3:100 in DRG medium.

Calibration of the laser trap

The laser optical trap was calibrated by viscous drag through the aqueous medium in the microscope focal plane (Kuo and Sheetz, 1993). The viscous force was generated by oscillatory motion of the specimen by a piezoceramic-driven stage (Wye Creek Instruments, Frederick, MD) at a constant velocity. The position of the bead in the trap was tracked using the nanometer-level tracking program (Gelles et al., 1988) to analyze video records of the experiments. Positional variation of the particle in the trap with 60 mW was 11 (± 1.7) nm. The calibration shows a very linear force-distance relationship for the optical tweezers (Fig. 1). To study the variation in trap calibration with height above the coverslip surface, latex beads (0.5 μm in diameter) were trapped with the same laser power at different perpendicular positions. The increase in particle displacement at 2 μm or less from the glass surface (Fig. 1 B) implies a viscous coupling to the coverslip surface. From 2–5 μm above the surface, the force on the beads in the trap was constant (Fig. 1 B). This calibration was used to calculate the forces that form tethers. All of these experiments were performed 3–4 μm above the coverslip surface to minimize viscous coupling to the glass surface, and the laser power was simultaneously monitored.

Laser optical trap manipulations

Just before observation, the cloning cylinder was removed and the coverslip containing the cells was mounted on an aluminum coverslip holder using silicone grease; then a second cleaned coverslip was mounted on top to form a flow cell. The IgG-covered latex beads and the treatment solutions such as cytochalasins and DMSO were exchanged for the normal medium. The growth cones were viewed by a video-enhanced differential interference contrast (DIC) microscope (IM-35 microscope; Zeiss, Oberkochen, Germany) with a fiber optic illuminator. The stage was maintained at 38°C using an air current incubator. The laser trap consisted of a polarized beam from an 11W TEM₀₀-mode near-infrared (1064 nm) laser (model C-95; CVI Corporation, Albuquerque, NM) that was expanded by a 3 \times beam expander (CVI Corporation) then focused through an 80-mm-focal-length achromatic lens (Melles Griot, Irvine, CA) into the epifluorescence port of the Zeiss IM-35 microscope (Kuo and Sheetz, 1992). In the binding experiments, the IgG-covered beads were added by exchange of the cell culture medium. The bead was trapped with ~ 60 mW of laser power, put on to the cell surface and held for 4 s before pulling at a constant velocity. To determine the probability of bound beads forming tethers, the beads were held with the laser trap on the cell surface for 4 s and were pulled out at a velocity of ~ 3 $\mu\text{m/s}$. We determined that the percentage of tether formation was not altered

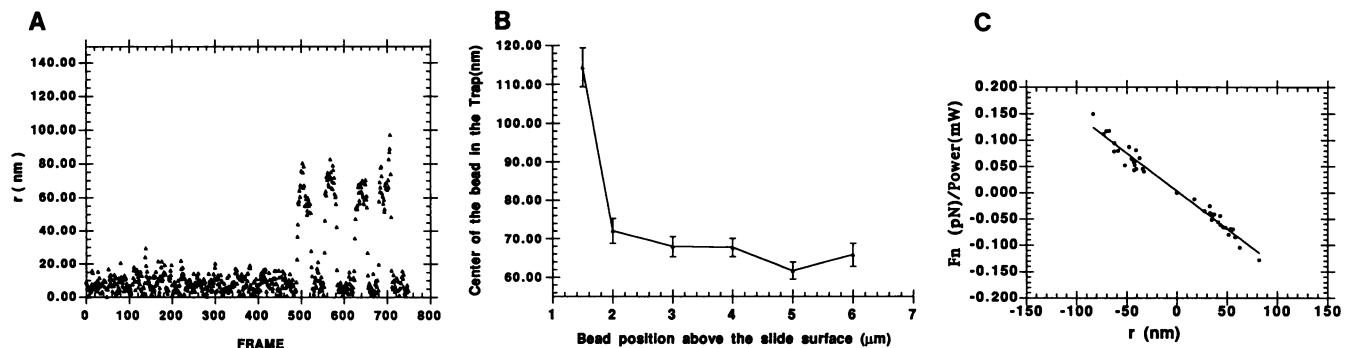


FIGURE 1 Sequence of measurements to calibrate the radial force of the trap. (A) The radial position of the bead (r) in the trap during a series of calibration displacements. The bead was held with the laser trap $\sim 4 \mu\text{m}$ above the coverslip surface, and the piezoceramic-driven stage was moved repeatedly at a constant rate. (B) Calibration of the laser trap at different heights above the glass surface. The displacement procedure in A was repeated for latex beads ($0.5 \mu\text{m}$ in diameter) held at different heights above the coverslip, at constant power. Six beads were tested at each height. The results show that experiments need to be done at least $2 \mu\text{m}$ above the coverslip surface to minimize viscous coupling to the glass surface. (C) Calibration of the laser trap for particles held $\sim 3\text{--}4 \mu\text{m}$ above the coverslip surface by varying the laser power for a constant velocity of movement. The result is shown as the relationship between the position of the bead in the trap (r) and the normalized light force F_N in pN mW^{-1} , as calculated from Stokes Law and the power of the trap, which was monitored simultaneously. The slope of the linear fit line is $1.443 (\text{pN } \mu\text{m}^{-1} \text{ mW}^{-1})$.

by exposing growth cones to even 10 s of laser irradiation. Beads either remained at the cell surface or a tether was formed. All of the samples treated or untreated were manipulated under the same conditions.

Analysis of the mechanical properties of the membranes

To measure the force of the tether at zero velocity, F_0 , the position of the bead in the trap during tether formation was tracked using the nanometer-scale tracking program that was developed previously (Gelles, 1988), and the force (F) of the tether on the bead was calculated from the calibration of the laser trap. After measuring the tether growth rate (V) using a "ruler" program, a plot F vs. V was obtained. Two methods were used to estimate the radius of the tether. First, latex beads $0.5 \mu\text{m}$ in diameter were used as a standard in the "ruler" program. From the video tape, we measured the relative diameter of the tether and then compared with the bead. The other way was to determine the relative intensity through orthogonal scans across the DIC image of both the tether and the axon (Schnapp et al., 1988). After measuring the diameter of the axon with the "ruler" program, we can estimate the radius of the tether (the intensity should be related to the radius squared). The radius of the tether was calculated to be about $0.2 \mu\text{m}$ in both cases. With increasing velocity, there was no detectable change in tether contrast. To calculate the membrane surface viscosity, we developed a program using the fourth-order Runge Kutta routine to solve the equation (Eq. 21) in Dr. Waugh's paper (Waugh, 1982a) and compared that value with the formulation described by Hochmuth and colleagues (Hochmuth et al., 1982a).

RESULTS

Probability of bead binding and tether formation

When the IgG-coated beads were held on the DRG growth cone surface with the optical tweezers for 4 s, only a fraction bound to the membrane. Those that did bind to the surface did so irreversibly and would not release under the conditions tested. Pulling on beads with the optical tweezers either produced tubular membrane tethers or the beads were pulled out of the tweezers. To understand the cellular factors that influence binding and tether formation, we measured the effect of the cytochalasins, nocodazole, ATP depletion (Sheetz

et al., 1990), and organic solvents (dimethylsulfoxide (DMSO) and ethanol) on the probability of binding and tether formation. As shown in Fig. 2, there was no change in the probability of bead binding with any of the changes in the cellular conditions.

We expected that the probability of tether formation would be related to the cytoskeleton-membrane interaction and that

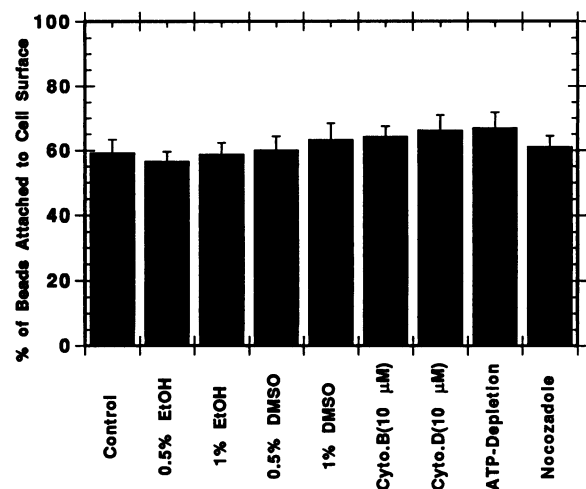


FIGURE 2 Bead binding to the surface is measured as the probability of IgG covered latex beads binding to the chicken DRG growth cone surface after 4 s using a laser trap of $\sim 60 \text{ mW}$ (laser power measured in the specimen plane) for a variety of experimental conditions. For the DMSO and ethanol (EtOH) treatment, DMSO or EtOH was added to the MEM medium, and the final concentration for DMSO or EtOH is 0.5 and 1%, respectively. Cytochalasin B and D were diluted into the MEM medium from DMSO stock solutions to give final concentrations for both Cytochalasin B and D of $10 \mu\text{M}$ and for DMSO of $\sim 0.3\%$. The nocodazole solution was prepared by diluting a 10 mM nocodazole stock solution in DMSO to give a $10 \mu\text{g/ml}$ solution. For ATP depletion, a solution of 2-deoxyglucose (30 mM) and sodium azide (10 mM) in the cell medium was used, and the growth cones assayed showed no motility. All of these treatment solutions were added to the cells by exchange flow, and the cells were incubated for 10 min before starting the measurements. For each experiment, 70 beads were studied.

the probability of tether formation would increase with the force of the tweezers (as was observed). On a related issue, those particles that did not form tethers normally did not diffuse after escaping from the trap, indicating that they were attached to the cytoskeleton. Because most factors were likely to decrease the affinity of the two structures, we chose a relatively low force (~ 10 pN) where only 36% of the beads would form tethers (Fig. 3). Cytochalasin B and D are known to inhibit actin dynamics within growth cones and cells, resulting in a condensation of the actin network and separation of the actin cytoskeleton from much of the membrane. Both cytochalasins increased the probability of tether formation to greater than 90%. Controls of the solvent (DMSO) used for adding the cytochalasins (0.25% solvent) also showed some increase, but 0.5% DMSO only increased the probability of tether formation to 55% (Fig. 3). Both the disruption of microtubules by nocodazole and the block of motility by ATP depletion caused no change in tether formation. Thus, changes in the organization of the actin cytoskeleton, but not microtubules or ATP levels, produced an increase in the ability to form tethers.

Static tether force (F_0)

After tethers are formed on DRG growth cones, they rapidly retract when the tweezers are turned off, indicating that a significant force is pulling the tether membrane back onto the growth cone. Photographs of the tether-pulling sequence are shown in Fig. 4, including bead binding to the cell surface in the trap, pulling the tether at a constant rate with the laser trap, and the complete retraction of the tether when the tweezers were turned off. We can utilize the measured displacement of the bead in the trap to estimate the force of the tether on the bead (Fig. 5 A). The tether force increases only slightly with the tether length in other systems where it has been

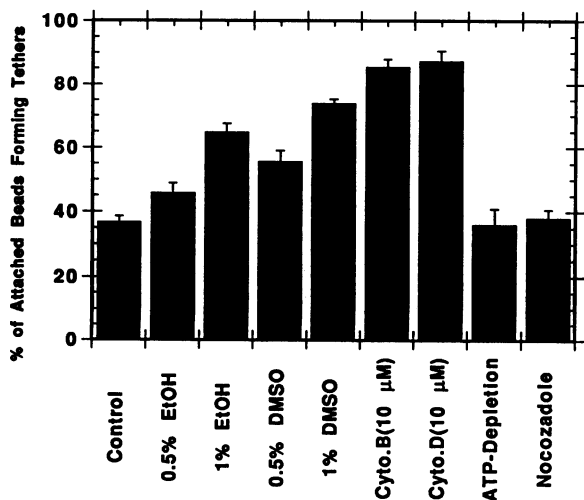


FIGURE 3 The probability of tether formation for the beads attached to the cell surface. The beads were pulled using the laser trap (60 mW) and at a constant velocity (3 μ m/s). The treatments are the same as described in Fig. 2. For each experiment, 50 beads were studied.

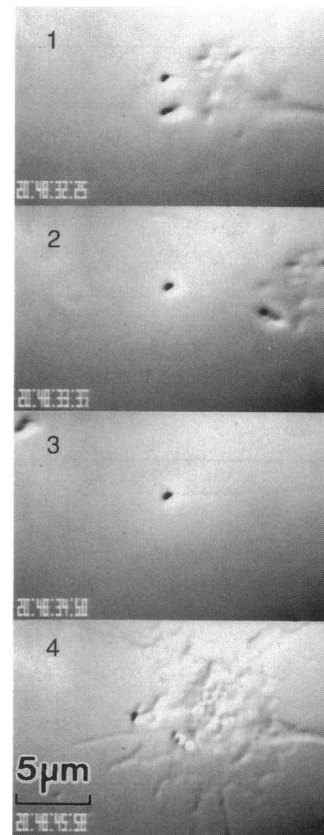


FIGURE 4 Photomicrographs of the tether-pulling sequence. (1) Bead was held on the growth cone surface by the laser trap. (2 and 3) The tether was pulled at a constant velocity by the laser trap. (4) The complete retraction of the tether when the laser trap was turned off.

tested (D. B. Wayne, S. C. Kuo, and M. P. Sheetz, unpublished data). The average tether length in the experiments was around 15 μ m. Rather we have measured the change in the tether force with the velocity of tether elongation and extrapolated to zero velocity to obtain a critical force, F_0 , which must be exceeded for tether growth. Where we tested it, the F_0 estimated from extrapolation to zero velocity was within experimental error of the value obtained in static measurements of the tether force.

Fig. 5 A shows the distance between the center of the bead and the center of the laser trap after the initial extension and then during a constant velocity elongation. In about 10 percent of the cases, the force peaked at the start of the elongation and then returned to a plateau level. For these studies we estimated the average plateau level for the force measurement. After plotting the force (F) forming the tether vs. the tether growth rate (V), we performed a linear least-squares fit and extrapolated to $V = 0$ to obtain F_0 (Fig. 5 B). The measurements for Fig. 5 were all made with different tethers that were formed on many different growth cones. For the control sample, we also measured the displacement of the beads at zero velocity and obtained an average value of this force of $5.0 (\pm 1.5)$ pN, which is in agreement with the estimation of F_0 from the F vs. V plot of 6.6 ± 0.3 ($N = 3$) pN.

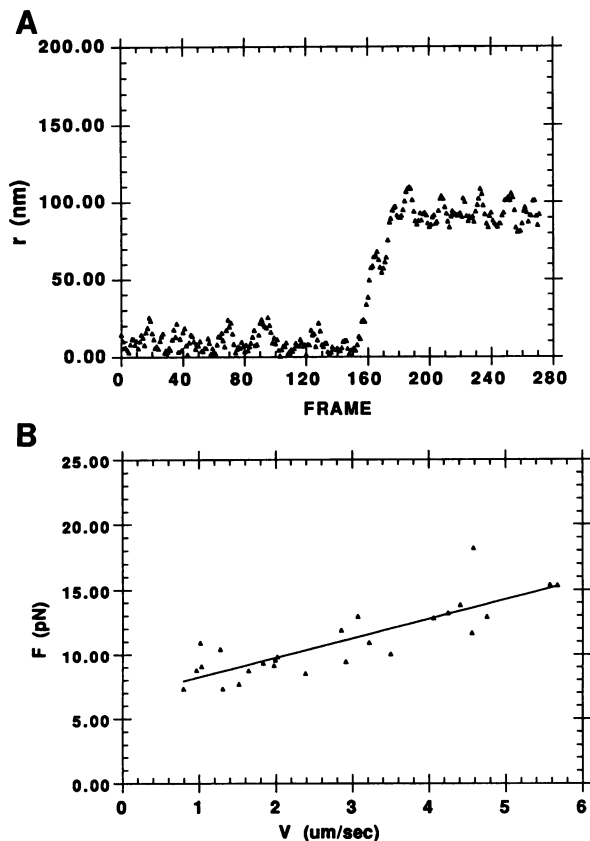


FIGURE 5 (A) The position of the bead in the trap (r) with time during the tether formation. After the bead was trapped, it was first held on the cell surface for ~ 5 s and then pulled out at a constant velocity, forming a tether. This tether length is $\sim 14 \mu\text{m}$. (B) Determination of the force (F_0) at zero velocity of tether growth from plotting F vs. tether growth rate (V). $F_0 = 6.72$ pN was obtained at $V = 0$ from a linear least-squares fit of the data points (slope of the plot = 1.51).

Because F_0 should reflect components of the in-plane tension of the plasma membrane and membrane bending rigidity, we expected that changes in the cellular organization should alter F_0 . When the growth cones were treated by cytochalasin B and D, ethanol, and DMSO, F_0 went from 6.7 pN down to ~ 3 pN in the presence of DMSO and to ~ 4 pN in the presence of cytochalasins and ethanol (Fig. 6 A). However, F_0 was not affected by nocodazole or ATP depletion. These results are similar to the probability of tether formation and suggest that the cytoskeleton plays a major role in determining the force needed to extend filopodia and tethers.

Viscous forces in tethers

As the velocity of tether elongation was increased, there was a linear increase in the force of the tether on the bead from the viscous components of membrane movement into the tether. There are several different analyses of the viscous components that contribute to the overall viscous force. Contributions could come from curving the membrane and the resulting interbilayer shear, from the bilayer viscosity, and from the drag of moving membrane past the associated cyto-

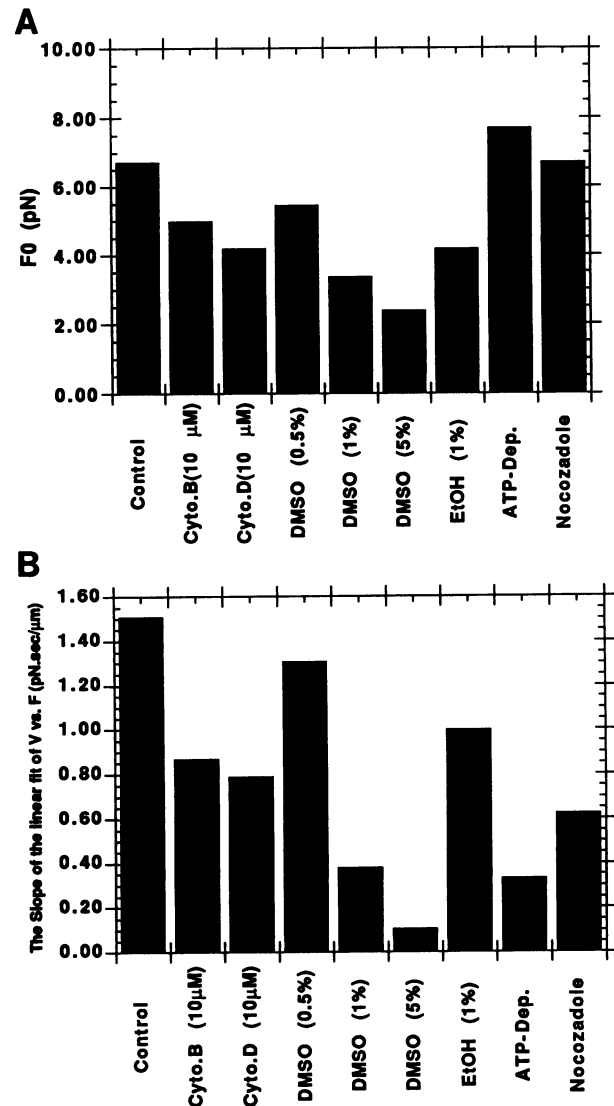


FIGURE 6 (A) The critical force (F_0) of the growth cones before and after various treatments. The treatment protocols are described in Fig. 2. (B) The slope derived from a linear least-squares fit of the tether growth rate vs. the force of tether formation. The coefficient of the correlation in each experiment in Fig. 6 is given below: (from control to nocodazole) 0.84, 0.81, 0.86, 0.82, 0.71, 0.89, 0.76, 0.66, and 0.60, respectively.

skeleton. Waugh's equation (Waugh, 1982a) allows us to estimate an apparent membrane viscosity neglecting contributions of the viscous shear between the cell membrane and cytoskeleton and the slip between halves of the bilayer (Fig. 7). Alternate methods of calculating the membrane viscosity include other viscous terms and, therefore, this value represents an upper limit of the membrane viscosity.

There were surprisingly large decreases in the slope with cytochalasin B and D, DMSO, and ATP depletion. The pattern of the viscosity changes with these treatments was not the same as changes in F_0 . The greatest difference was with ATP depletion. Compared with the control sample, F_0 is a little bit bigger but the slope is about 3 times smaller after the ATP depletion (Fig. 6 B). Thus, the viscous properties of

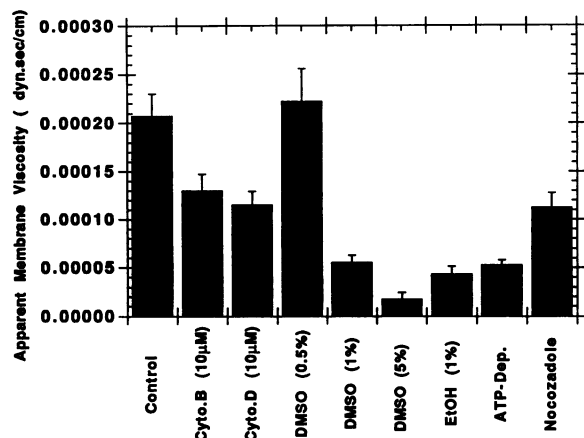


FIGURE 7 The apparent membrane surface viscosity of the growth cones before and after the treatments. The viscosity was estimated following Eq. 21 in Waugh (1982).

the growth cone membranes are dramatically altered by metabolic and cytoskeletal changes.

DISCUSSION

The optical tweezers have been proven useful for a number of studies of motor function and a wide variety of biological experiments (Kuo and Sheetz, 1992, 1993; Svoboda and Block, 1994; Finer et al., 1994). Here we show that they can be used to provide a relative measure of membrane-cytoskeleton attachment and the mechanical properties of membranes. The limitation of the tweezers is photodamage, and we have been concerned that photodamage may influence the values obtained. From our experience with DRG growth cones, there is no observable change in growth cone behavior at these trap levels, whereas at higher irradiation levels (>200 mW) we do observe loss of filopodia and a general inhibition of motility. An additional problem is the potential for forming tethers without beads, but such tethers are notably different in that they contain a bulb of cytoplasm at the end (Ashkin and Dziedzic, 1989). Further, without beads we were unable to form tethers at the laser powers used. The trap could exert some force directly on the tether, but it is considerably smaller in diameter (~200 nm vs. 500 nm for the bead) and further separated from the trap center, which makes it unlikely that the direct force on the tether is more than 20% of that on the bead. For comparing the relative forces under different cellular conditions, the optical tweezers provides self-consistent measurements, and the measured forces represent a lower bound for the actual values.

Membrane-cytoskeleton attachment

The exact nature of the linkages between membranes and the cytoskeleton are still ambiguous, although two general types of linkage have been considered. In one case, attachments would arise from transmembrane glycoproteins that are ultimately linked to actin-binding proteins. Alternatively, cy-

toskeletally linked proteins such as spectrin could weakly associate with the bilayer surface and, because such proteins are in an extended configuration and part of larger complexes, the sum of the many weak interactions would form a strong linkage. In macroscopic terms, the difference here is similar to that between a soap membrane covering but only tied at a few discreet points to a rigid structural net and a soap film spread across that same net where it is adsorbed to elements of the net. In the first instance, the disruption of the structural net (most likely actin-based) would make it easier to separate the membrane from the net; but the force, F_0 , needed to hold the membrane off the net should not change. In the second case, alteration of the net should affect both the ease of separation of the membrane from the net; and because the membrane-net association is reversible, it should also affect the force, F_0 , needed to hold the two structures apart. We find that both the percent tether formation and F_0 are altered in parallel, which is most consistent with the latter hypothesis, namely, that the attachments that prevent tether formation are reversible and contribute to the tension in the tether or F_0 .

There are several other reasons to believe that the membrane is not extensively tied to the cytoskeleton by strong contacts. Recent estimates of the mechanical force required to break apart a protein-protein interaction with a 10^{-5} association constant are large, in the range of 10 pN (Kuo and Lauffenburger, 1993). Breaking of such interactions would result in a dramatic decrease in the force on the bead. Although jumps are seen occasionally at the start of tether formation, they are small in magnitude, 6–10 pN, and are only seen in ~10% of tethers formed. From many previous studies of the diffusion of particles on the surface of growth cones and motile cells, barriers to lateral diffusion are spaced over micron distances (de Brabander et al., 1991; Edidin et al., 1991). We might expect a similar separation between the structural links that would hold the membrane and cytoskeleton together. Thus, with 0.5 micron beads, bound beads should be able to fit within the gaps in the network and tethers could be formed by pulling on those beads without breaking strong membrane-cytoskeletal linkages.

Previous studies have indicated that the probability of tether formation is inversely related to the membrane-cytoskeleton interaction (Schmidt et al., 1993). We know that both cytochalasins B or D can affect the network of actin filaments in the cell, although there is some small difference between them (Edds, 1993). DMSO can also affect the arrangement of cytoskeleton (Yumura and Fukui, 1983; Weiner et al., 1993). It has been reported that ethanol can influence cell migration and invasion in vitro as well as F-actin organization, and it can affect the membrane conformation and structure (Weiss et al., 1991; Mooradian and Smith, 1993; Staler et al., 1993; Ho et al., 1994). Therefore, a possible explanation for the above result is that the cytochalasins and DMSO will decrease the membrane-cytoskeleton interaction through rearrangements of the actin cytoskeleton and thereby increase the probability of tether formation for a given force. On the other hand, DMSO, like

ethanol, might indirectly affect membrane mechanics through an alteration in the interfacial interaction energy between the membrane and an otherwise normal actin cytoskeleton. The microtubule (MT) organization in cells appears to have no effect on the membrane-cytoskeleton interaction (Wang et al., 1993) as does ATP depletion. In other growth cones, ATP depletion inhibits the particle movement on the membrane (Sheetz et al., 1990). General alteration in the organization of the actin cytoskeleton is linked to parallel changes in the probability of tether formation and F_0 . We suggest that the membrane interaction with the cytoskeleton is through reversible, weak bonds and not through strong protein-protein bonds.

F_0 of growth cone membranes (~ 6.7 pN) is much less than that of erythrocyte membranes, which is about 50 pN (Waugh and Bauserman, 1995, in press). The larger membrane tension of the preswollen red cells might contribute the larger F_0 . There is an extensive interaction between the red cell spectrin-actin network and the membrane bilayer that possibly accounts for the major portion of the force required for tether extension. By implication, a similar network may be associated with the growth cone plasma membrane. In comparison with the forces that myosin motors or actin polymerization can develop, the force for extension is comparable with two myosin molecules or one actin filament, indicating that either mechanism could generate sufficient force to produce extension (Sheetz, 1994). In addition to binding force between membrane and cytoskeleton, other factors that contribute to the force required for tether formation include the membrane bending stiffness and the in-plane membrane tension (Hochmuth, personal communication). The bending stiffness of the membrane plays an important role in processes because of the major changes in membrane curvature. To estimate the membrane bending stiffness, an equation developed by Waugh and Hochmuth (1987) can be used. In this case, if we assume that the force (F) forming the tether is 8 pN, the radius (r_t) of the tether is $0.2 \mu\text{m}$, then the bending stiffness (B) = $F \times r_t / 2\pi = 2.55 \times 10^{-12}$ dyne cm. The growth cone membrane bending stiffness is similar to that of the lipid bilayer membranes $\sim 1.0\text{--}2.5 \times 10^{-12}$ dyne cm. (BO and Waugh, 1989) and erythrocyte membranes (Evans, 1983). Because the bending stiffness of the bilayer should not change with cytochalasin B or D, we suggest that the reversible membrane cytoskeleton associations or possibly in-plane tension is decreased by these treatments.

Membrane surface viscosity

The viscoelastic properties of the membrane could contribute to the control of growth and extension rates, but these data indicate that viscous forces are too small at typical extension velocities (maximally $0.03\text{--}0.25 \mu\text{m/s}$) to cause a significant effect. Although there are potentially several factors contributing to the viscoelastic force, we have used Eq. 21 in Waugh's paper (Waugh, 1982a) to estimate the membrane viscosity. Because the growth cone is only a very small part

of the whole neuron cell, the ratio of the radius of the tether (r_t) ($\sim 0.2 \mu\text{m}$) to the radius of the cell (r_c) or (r_t/r_c) is very small ($<1/50$). Following Waugh, the value of F/F_0 can be used directly to calculate membrane surface viscosity (Waugh, 1982a), which is about 2.1×10^{-4} dyn s/cm (Fig. 7). In these studies, the apparent viscosity ranged from 0.56×10^{-4} to 4.2×10^{-4} dyn s/cm. This value is much smaller than that Hochmuth obtained for erythrocyte membranes (2.8×10^{-3} dyn s/cm) and is greater, perhaps very significantly, than that reported for egg phosphatidylcholine large bilayer vesicle membranes ($\sim 1.7 \times 10^{-4}\text{--}5.0 \times 10^{-6}$ dyn s/cm) (Hochmuth et al., 1982b; Waugh, 1982b).

Which of the factors, including the slippage of membrane layers in moving to a highly curved surface, the planar membrane viscosity, and glycoprotein collisions with the cytoskeleton, makes the major contribution to the viscosity during extension flow is unclear. Evans suggested that the slope of the linear fit of the tether growth rate (V) vs. the force (F) forming tethers should be related to the friction in the slipping of the bilayers past one another as the bilayer moves from the flat membrane surface to the highly curved tether (E. A. Evans, Personal communications). Because we see a major effect of the cytochalasins on viscosity and they should have little effect on the interface between the two bilayer halves, we consider that this factor makes only a small contribution to the control of membrane viscosity. There is a large difference between the viscosity of the neuronal membrane and the liposome or red cell membranes using the same formula. Current models of membrane viscosity are being challenged because they lack terms to consider the slippage between the two bilayer halves and cytoskeletal contributions; thus, better models of this system are needed to provide testable hypotheses. It is somewhat surprising to find such large changes in the viscosity with alteration of cell cytoskeleton and particularly with ATP depletion.

Axon elongation and tether formation

An interesting question in axon elongation is: where does the axon membrane come from? In these studies, we are forming tethers at a very rapid rate and lipid is flowing onto the tether at 10–100 times the rate that membrane moves into axons (typical axon elongation rates are $1\text{--}4 \mu\text{m/min}$, and diameters are typically 1 micron, whereas we are pulling tethers of 0.4 micron at rates of $60\text{--}600 \mu\text{m/min}$). Because the forces needed to produce such rapid extensions are considerably less than those developed by growth cones moving on normal substrata, it should be no problem for growth cones to pull membrane from the cell body and no need to invoke addition at the growth cone (Bray and Chapman, 1985; Popov et al., 1993). In the studies of erythrocyte membranes and liposome membranes, the membranes forming tethers were all from the surface membranes, but in active growth cones, some of the membrane might come from the cell body or from internal membrane vesicles. We consider this last possibility less likely because normally endocytosis and exocytosis are balanced and we are pulling at such a high rate that we would

not expect acute adaptation by membrane fusion. Rather, there appears to be a reservoir of membrane that the tethers draw upon either through alteration of the growth cone geometry or from stretching the membrane.

There are a number of biological processes for which tether data are relevant, including cell migration, cell volume, and membrane area regulation. The probability of tether formation relates to the ability of the cells to migrate because the release of cell contacts in the rear of the cell often involves formation of retraction fibers, i.e., tethers (Schmidt et al., 1993). How the cell regulates its surface area and the related parameter of cell volume may well involve an in-plane membrane tension that would regulate endocytic versus exocytic rates. Clearly, cytoskeletal factors do affect the physical parameters of tether formation, implying that they are important for cellular functions.

SUMMARY

Growth cone migration is accompanied by dramatic morphological changes and an extension of the axonal membrane. From our analyses of the mechanical properties of the membranes, we find that the forces generated by the membrane are on the order of those generated by a few myosin motors or actin polymerization or from the breaking of weak protein-protein interactions. Because membrane-cytoskeleton interactions influence the probability of tether formation and the critical force required to extend a membrane tether, we suggest that the interactions between the membrane and the skeleton are weak and reversible, although pointwise strong interactions cannot be excluded. The viscous properties of the tethers show a strong dependence on solvents and ATP depletion that are not understood. Thus, we find that the laser tweezers can be used to assay the strength of the interaction between the cytoskeleton and the membrane bilayer that in turn can influence cell migratory behavior.

We thank Drs. Evans and Hochmuth for their helpful comments on this work. We also thank our colleagues Denise Wayne, Zhaoxue Wang, Mingya Jiang, Hanry Yu, and Ron Sterba for their kind help or helpful discussion in part of this work.

This work was supported by grants from National Institutes of Health, Human Frontier Science Program, and Muscular Dystrophy Association.

REFERENCES

- Ashkin, A. 1970. Acceleration and trapping of particles by radiation pressure. *Phys. Rev. Lett.* 24:156–159.
- Ashkin, A. 1992. Forces of a single-beam gradient laser trap on a dielectric sphere in the ray optics regime. *Biophys. J.* 61:569–582.
- Ashkin, A., and J. M. Dziedzic. 1987. Optical trapping and manipulation of viruses and bacteria. *Science*. 235:1517–1520.
- Ashkin, A., and J. M. Dziedzic. 1989. Internal cell manipulation using infrared laser traps. *Proc. Natl. Acad. Sci. USA*. 86:7914–7918.
- Ashkin, A., J. M. Dziedzic, J. E. Bjorkholm, and S. Chu. 1986. Observation of a single-beam gradient force optical trap for dielectric particles. *Optics Lett.* 19:288–290.
- Ashkin, A., J. M. Dziedzic, and T. Yamane. 1987. Optical trapping and manipulation of single cells using infrared laser beams. *Nature*. 330:769–771.
- Bennett, V. 1990. Spectrin-based membrane skeleton: a multipotential adaptor between plasma membrane and cytoplasm. *Physiol. Rev.* 70:1029–65.
- Berk, D. A., and R. M. Hochmuth. 1992. Lateral mobility of integral proteins in red blood cell tethers. *Biophys. J.* 61:9–18.
- Bo, L., and R. E. Waugh. 1989. Determination of bilayer membrane bending stiffness by tether formation from giant, thin-walled vesicles. *Biophys. J.* 55:509–517.
- Bray, D., and K. Chapman. 1985. Analysis of microspike movements on the neuronal growth cone. *J. Neurosci.* 5:3204–3213.
- Bray, D., J. Heath, and D. Moss. 1986. The membrane-associated “cortex” of animal cells: its structure and mechanical properties. *J. Cell Sci. Suppl.* 4:71–88.
- Bretscher, M. S. 1989. Endocytosis and recycling of the fibronectin receptor in CHO cells. *EMBO J.* 8:1341–1348.
- Cooper, J. A. 1991. The role of actin polymerization in cell motility. *Annu. Rev. Physiol.* 53:585–605.
- Debrabander, M., R. Nuydens, A. Ishihara, B. Holifield, K. Jacobson, and H. Geerts. 1991. Lateral diffusion and retrograde movements of individual cell surface components on single motile cells observed with nanovid microscopy. *J. Cell Biol.* 112:111–124.
- Eddidin, M., S. Kuo, and M. P. Sheetz. 1991. Lateral movements of membrane glycoproteins restricted by dynamic cytoplasmic barriers. *Science*. 254:1379–1382.
- Eddidin, M., M. C. Zuniga, and M. P. Sheetz. 1994. Truncation mutants define and locate cytoplasmic barriers to lateral mobility of membrane glycoproteins. *Proc. Natl. Acad. Sci. USA*. 91:3378–3382.
- Edds, K. T. 1993. Effects of cytochalasin and colcemid on cortical flow in coelomocytes. *Cell Motil. Cytoskel.* 26:262–273.
- Evans, E. A. 1983. Bending elastic modulus of red cell membrane derived from buckling instability in micropipette aspiration tests. *Biophys. J.* 43:27–30.
- Evans, E. A., and R. Skalak. 1979. Mechanics and thermodynamics of biomembranes. *CRC Crit. Rev. Bioeng.* 3:181–418.
- Finer, J. T., R. M. Simmons, and J. A. Spudich. 1994. Single myosin molecule mechanics: piconewton forces and nanometer steps. *Nature*. 368:113–119.
- Gelles, J., B. J. Schnapp, and M. P. Sheetz. 1988. Tracking kinesin-driven movements with nanometer-scale precision. *Nature*. 331:450–453.
- Gordon-Weeks, P. R. 1991. Control of microtubule assembly in growth cones. *J. Cell Sci. Suppl.* 15:45–49.
- Ho, C., B. W. Williams, M. B. Kelly, and C. D. Stubbs. 1994. Chronic ethanol intoxication induces adaptive changes at the membrane protein/lipid interface. *Biochim. Biophys. Acta*. 1189:135–142.
- Hochmuth, R. M., and E. A. Evans. 1982a. Extensional flow of erythrocyte membrane from cell body to elastic tether. I. Analysis. *Biophys. J.* 39:71–81.
- Hochmuth, R. M., N. Mohandas, and P. L. Blackshear. 1973. Measurement of the elastic modulus for red cell membrane using a fluid mechanical technique. *Biophys. J.* 13:747–762.
- Hochmuth, R. M., H. C. Wiles, E. A. Evans, and J. T. McCown. 1982b. Extensional flow of erythrocyte membrane from cell body to elastic tether. II. Experiment. *Biophys. J.* 39:83–89.
- Kucik, D. F., S. C. Kuo, E. L. Elson, and M. P. Sheetz. 1991. Preferential attachment of membrane glycoproteins to the cytoskeleton at the leading edge of lamella. *J. Cell Biol.* 114:1029–1036.
- Kuo, S. C., and D. A. Lauffenburger. 1993. Relationship between receptor/ligand binding affinity and adhesion strength. *Biophys. J.* 65:2191–2200.
- Kuo, S. C., and M. P. Sheetz. 1992. Optical tweezers in cell biology. *Trends Cell Biol.* 2:116–118.
- Kuo, S. C., and M. P. Sheetz. 1993. Force of single kinesin molecule measured with optical tweezers. *Science*. 260:232–234.
- Misawa, H., M. Koshioka, K. Sasaki, N. Kitamura, and H. Masuhara. 1990. Laser trapping, spectroscopy and ablation of a single latex particle in water. *Chem. Lett.* 8:1479–1482.
- Mooradian, A. D., and T. L. Smith. 1993. Membrane disordering effect of ethanol cerebral microvessels of aged rats: a brief report. *Neurobiol. Aging*. 14:229–232.
- Pasternak, C., and E. L. Elson. 1985. Lymphocyte mechanical response triggered by cross-linking surface receptors. *J. Cell Biol.* 100:860–872.

- Popov, S., A. Brown, and M. M. Poo. 1993. Forward plasma membrane flow in growing nerve processes. *Science*. 259:244–246.
- Schmidt, C. E., T. Chen, and D. A. Lauffenburger. 1994. Simulation of integrin-cytoskeleton interactions in migrating fibroblasts. *Biophys. J.* 67:461–474.
- Schmidt, C. E., A. F. Horwitz, D. A. Lauffenburger, and M. P. Sheetz. 1993. Integrin-cytoskeleton interactions in migrating fibroblasts are dynamic, asymmetric, and regulated. *J. Cell Biol.* 123:977–991.
- Schnapp, B. J., J. Gelles, and M. P. Sheetz. 1988. Nanometer-scale measurements using video light microscope. *Cell Motil. Cytoskel.* 10:47–53.
- Seeger, S., S. Monajembashi, K.-J. Hutter, G. Futterman, J. Wolfrum, and K. O. Greulich. 1991. Application of laser optical tweezers in immunology and molecular genetics. *Cytometry*. 12:497–504.
- Sheetz, M. P. 1993. Glycoprotein motility and dynamic domains in fluid plasma membranes. *Annu. Rev. Biophys. Biomol. Struct.* 22:417–31.
- Sheetz, M. P. 1994. Cell migration by graded attachment to substrates and contraction. *Semin. Cell Biol.* 5:149–155.
- Sheetz, M. P., N. L. Baumrind, D. B. Wayne, and A. L. Perlman. 1990. Concentration of membrane antigens by forward transport and trapping in neuronal growth cones. *Cell*. 61:231–241.
- Schut, T. C., G. Hesselink, B. C. De Grooth, and J. Greve. 1991. Experimental and theoretical investigations on the validity of the geometrical optics model for calculating the stability of optical traps. *Cytometry*. 12:479–485.
- Staler, S. J., C. Ho, F. J. Taddeo, M. B. Kelly, and C. D. Stubbs. Contribution of hydrogen bonding to lipid-lipid interactions in membranes, and the role of lipid order: effects of cholesterol, increased phospholipid unsaturation, and ethanol. *Biochemistry*. 32:3714–3721.
- Steubing, R. W., S. Cheng, W. H. Wright, Y. Numajiri, and M. W. Berns. 1991. Laser induced cell fusion in combination with optical tweezers: the laser cell fusion trap. *Cytometry*. 12:505–510.
- Svoboda, K., and S. M. Block. 1994. Biological applications of optical forces. *Annu. Rev. Biophys. Biomol. Struct.* 23:247–285.
- Trinkaus, J. B. 1985. Protrusive activity of the cell surface and the initiation of the cell movement during morphogenesis. *Exp. Biol. Med.* 10:130–173.
- Vasiliev, J. M. 1985. Spreading of non-transformed and transformed cells. *Biochim. Biophys. Acta*. 780:21–65.
- Wang, N., J. P. Butter, and D. E. Ingber. 1993. Mechanotransduction across the cell surface and through the cytoskeleton. *Science*. 260:1124–1127.
- Waugh, R. E. 1982a. Surface viscosity measurements from large bilayer vesicle tether formation. I. Analysis. *Biophys. J.* 38:19–27.
- Waugh, R. E. 1982b. Surface viscosity measurements from large bilayer vesicle tether formation. II. Experiments. *Biophys. J.* 38:29–37.
- Waugh, R. E., and R. M. Hochmuth. 1987. Mechanical equilibrium of thick, hollow, liquid membrane cylinders. *Biophys. J.* 52:391–400.
- Wayne, D. B., S. C. Kuo, and M. P. Sheetz. 1991. Actin polymerization rates in novel membranous extensions (neopodia) formed on neuronal growth cones. *J. Cell Biol.* 115:102a. (Abstr.)
- Weiner, O. H., J. Murphy, G. Griffiths, M. Schleicher, and A. A. Noegel. 1993. The actin-binding protein (p24) is a component of the Golgi apparatus. *J. Cell Biol.* 123:23–34.
- Weiss, L., B. B. Asch, and G. ELkin. 1991. Effects of cytoskeletal perturbation on the sensitivity of Ehrlich ascites tumor cell surface membranes to mechanical trauma. *Invasion & Metastasis*. 11:93–101.
- Wright, W. H., G. J. Sonek, Y. Tadir, and M. W. Berns. 1990. Laser trapping in cell biology. *IEEE J. Quant. Elect.* 26:2148–2157.
- Yumura, S., and Y. Fukui. 1983. Filopodelike projections induced with dimethyl sulfoxide and their relevance to cellular polarity in Dictyostelium. *J. Cell Biol.* 96:857–865.
- Zigmond, S. H. 1991. Recent quantitative studies of actin filament turnover during cell locomotion. *Cell Motil. Cytoskel.* 25:309–316.